

**The XXIV International Workshop
High Energy Physics and Quantum Field Theory
September 22 – September 29, 2019
Sochi, Russia**

Correlation femtoscopy at NICA energies

P. Batyuk¹, O.Kodolova², L. Malinina^{1,2}, K. Mikhaylov^{1,3},
G.Nigmatkulov⁴, G.Romanenko²

¹*Joint Institute for Nuclear Research, Dubna, Russia,*

²*Skobeltsyn Research Institute of Nuclear Physics, Moscow State University, Moscow, Russia,*

³*NRC Kurchatov Institute – ITEP, Russian Federation, Moscow, Russia,*

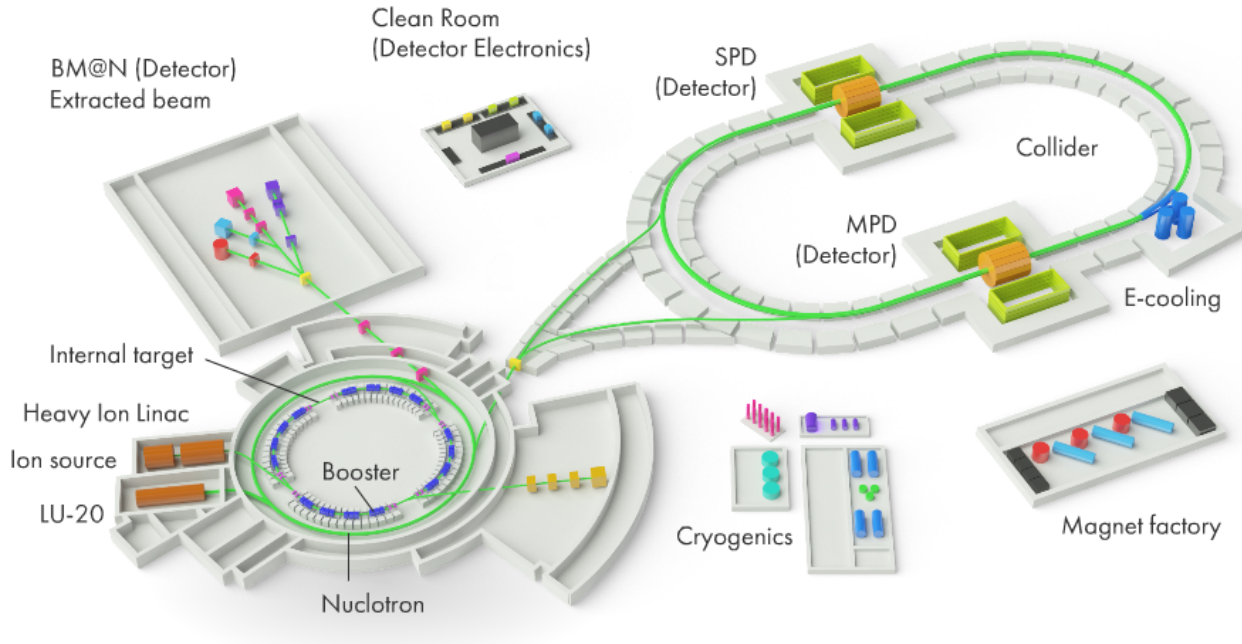
⁴*National Research Nuclear University, Moscow Engineering Physics Institute, Moscow, Russia.*

This work has been supported by the RFBR grant № 18-02-40044

Outline

- NICA
- Femtoscopy and Motivation
- Hybrid vHLLE+UrQMD model
- Comparison with STAR BES
 - pions
 - first results with kaons
- Conclusion

NICA complex



Beams - p, d ... $^{197}\text{Au}^{79+}$

Collision energy:

$$\sqrt{s_{\text{NN}}} = 4 - 11 \text{ GeV } E_{\text{lab}} = 1 - 6 \text{ AGeV}$$

$$\text{Luminosity: } 10^{27} \text{ cm}^{-2}\text{s}^{-1} (\text{Au}), \\ 10^{32} (\text{p})$$

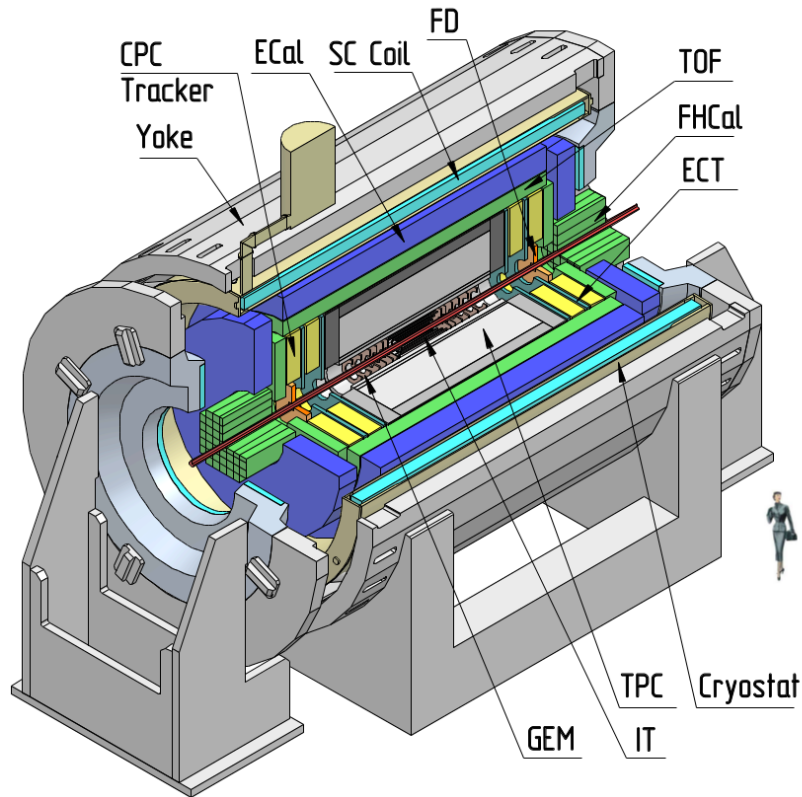
Specific scope elements of the project
NICA/MPD facility are expected to include:

- Injection complex,
- New superconducting Booster synchrotron,
- The existing superconducting heavy ion synchrotron Nuclotron,
- Collider having two new superconducting storage rings,
- New beam transfer channels.

- 2 interaction points - **MPD** and **SPD**
- Fixed target experiment - **BM@N**

- **2018**: extracted beams of heavy ions (Ar, Kr) are available within the BM@N experiment
- **2020-2021**: a first configuration of the MPD setup available.
- **2023**: commissioning of the fully designed NICA-complex is foreseen.

MultiPurpose Detector (MPD) for A+A collisions @ NICA



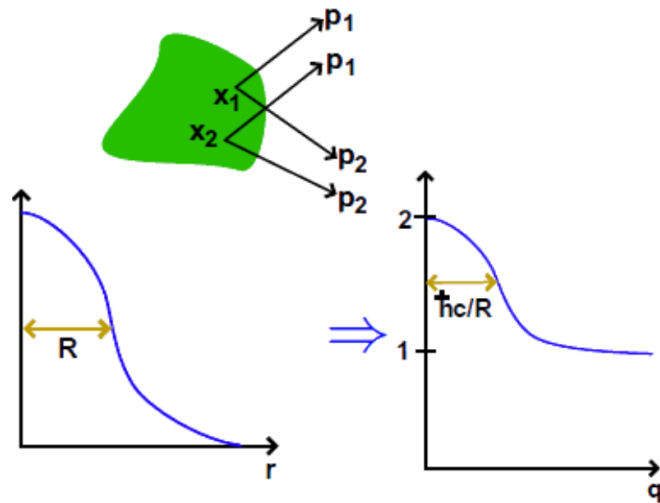
Benefits:

- Hermeticity, 2π -acceptance in azimuth
- 3D-tracking (TPC, ECT)
- Vertex high-resolution (IT)
- Powerful PID (TPC, TOF, ECAL)
 - π , K up to 1.5 GeV/c
 - K, p up to 3 GeV/c
 - γ , e from 0.1 GeV/c up to 3 GeV/c
- Precise event characterization (FHCAL)
- Fast timing and triggering (FFD)
- Low material budget
- High event rate (up to 7 kHz)

Realization progress:

- TDR - completed
- Detector mass production is on going
- First stage - 2021 (ready for cosmics - end of 2020)
- Second stage and full commissioning (IT + end-cups) - 2023

Femtoscscopy



Correlation femtoscopy :

Measurement of space-time characteristics \mathbf{R} , $\mathbf{c\tau}$ of particle production using particle correlations due to the effects of quantum statistics (QS) and final state interactions (FSI)

Two-particle correlation function:

theory:

$$C(q) = \frac{N_2(p_1, p_2)}{N_1(p_1) \cdot N_2(p_1)}, C(\infty) = 1$$

experiment:

$$C(q) = \frac{S(q)}{B(q)}, q = p_1 - p_2$$

$S(q)$ – distribution of pair momentum difference from same event

$B(q)$ – reference distribution built by mixing different events

Parametrizations used:

1D CF: $C(q_{inv}) = 1 + \lambda e^{-R^2 q_{inv}^2}$

R – Gaussian radius in PRF,

λ – correlation strength parameter

3D CF: $C(q_{out}, q_{side}, q_{long}) = 1 + \lambda e^{-R_{out}^2 q_{out}^2 - R_{side}^2 q_{side}^2 - R_{long}^2 q_{long}^2}$

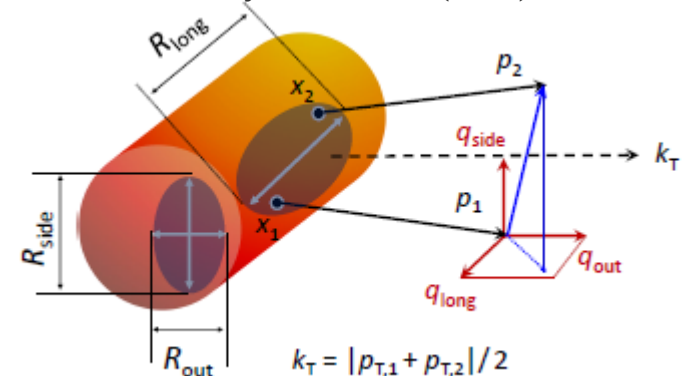
R and q are in Longitudinally Co-Moving Frame (LCMS)

long || beam; out || transverse pair velocity \mathbf{v}_T ; side normal to out, long

LCMS decomposition:

S. Pratt. Phys. Rev. D 33 (1986) 1314

G. Bertsch. Phys. Rev. C 37 (1988) 1896



Motivation

- **Femtосcopy allows one:**

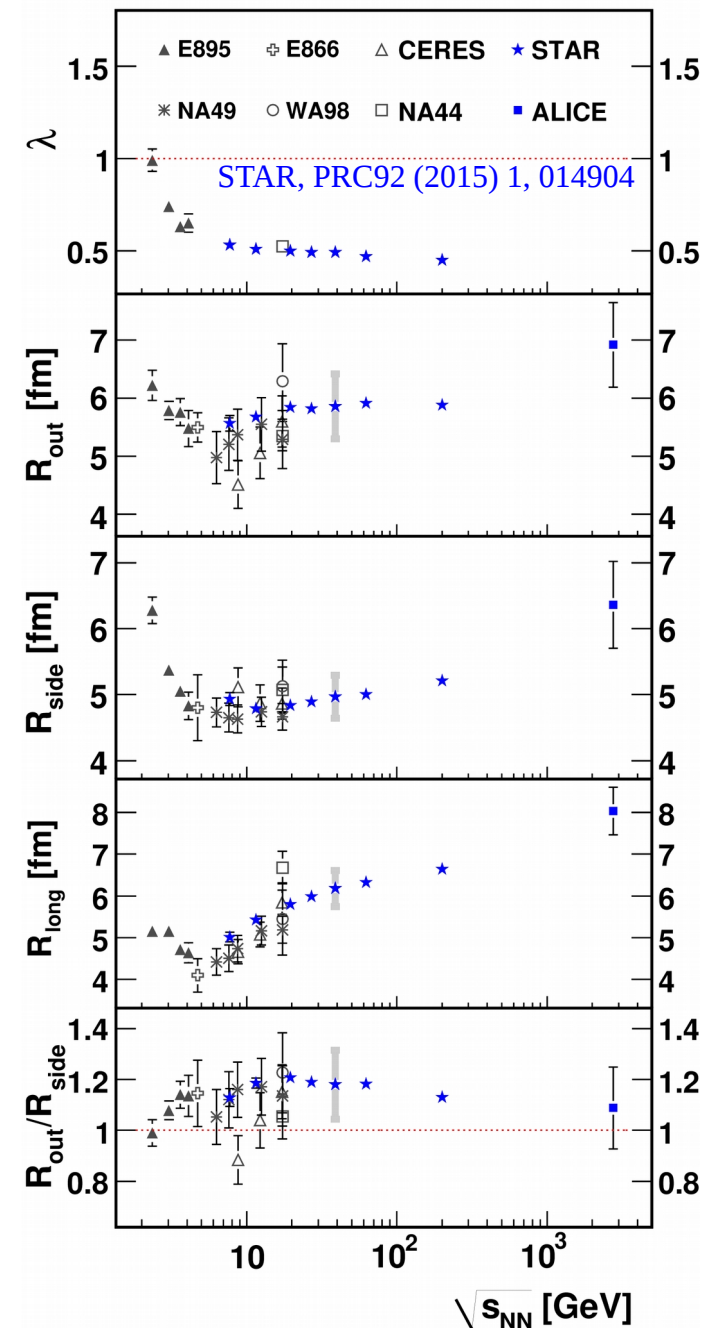
- To obtain spatial and temporal information on particle-emitting source at kinetic freeze-out
- To study collision dynamics depending on EoS

- **RHIC Beam Energy Scan program (BES-I):**

$$\sqrt{s_{NN}} = 7.7, 11.5, 19.6, 27, 39 \text{ GeV}$$

- The search for the onset of a first-order phase transition in Au + Au collisions
- Measured pion and kaon femtoscopic parameters:
 - m_T -dependence of radii,
 - flow-induced $x - p$ correlations

- NICA energy range: $\sqrt{s_{NN}} = 4 - 11 \text{ GeV}$
measurements with great accuracy

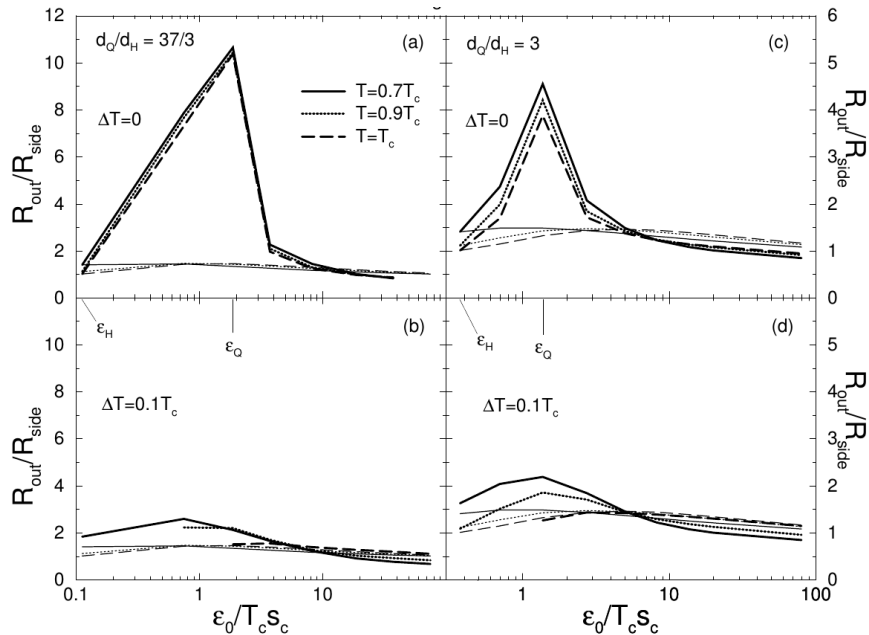


Expected features of first-order phase transition (1PT)

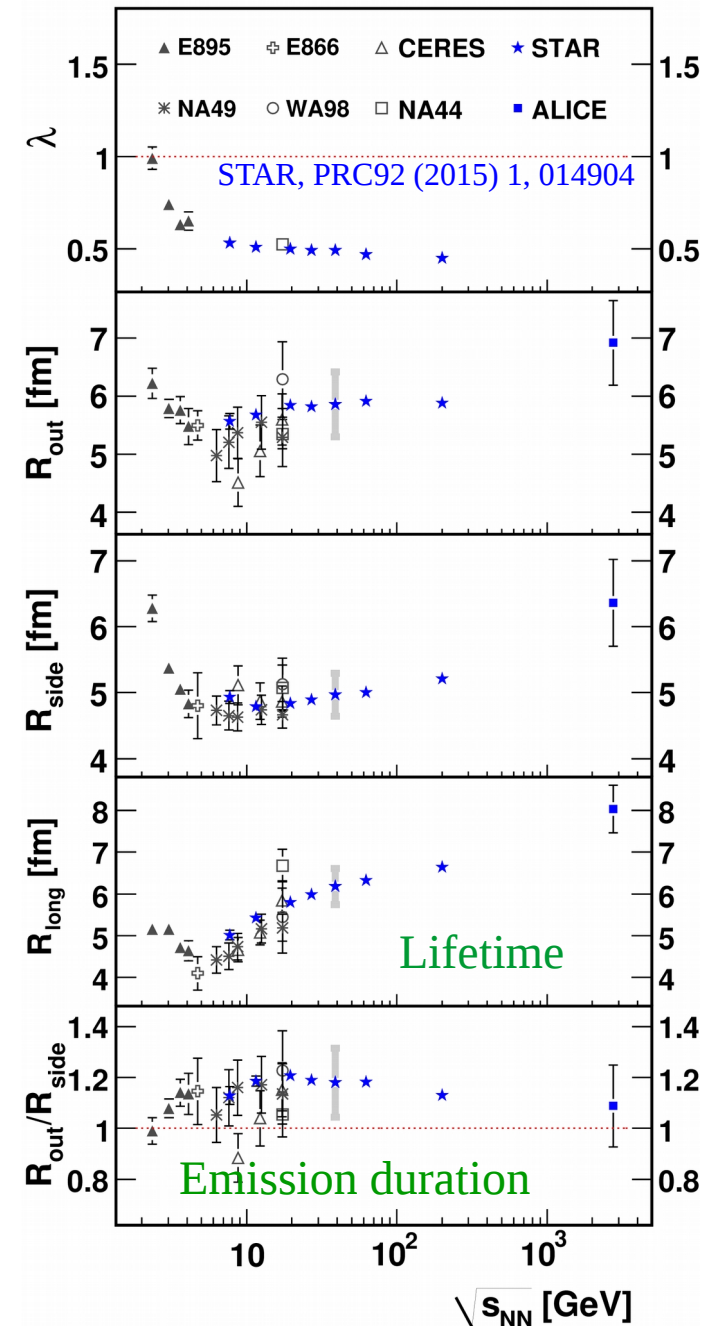
- It was predicted for first-order phase transition $R_{out}/R_{side} \gg 1$ and larger R_{long} due to emission stalling during phase transition.

S. Pratt, Phys. Rev. D 33 (1986) 1314. G. Bertsch, M. Gong, M. Tohyama, Phys. Rev. C 37 (1988) 1896

D. H. Rischke, M. Gyulassy, Nucl. Phys. A608, 479 (1996):

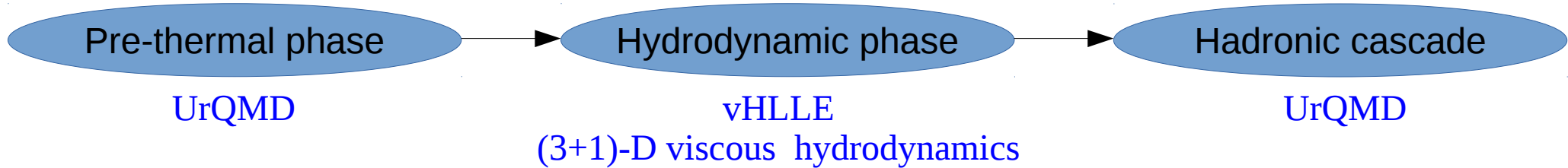


- But space-time correlations in expanding source reduce the observed $R_{out} \rightarrow R_{out}/R_{side}$
- Study of femtoscopy observables allows to perform tune of the models to describe correctly collision dynamics



Femtoscscopy with vHLLE+UrQMD

Iu. Karpenko, P. Huovinen, H.Petersen, M. Bleicher, Phys.Rev. C 91, 064901 (2015)



Parameters τ_0 , R_{\perp} , R_{η} and η/s adjusted using basic observables in the RHIC BES-I region.

$\sqrt{s_{NN}}$ [GeV]	τ_0 [fm/c]	R_{\perp} [fm]	R_{η} [fm]	η/s
7.7	3.2	1.4	0.5	0.2
8.8 (SPS)	2.83	1.4	0.5	0.2
11.5	2.1	1.4	0.5	0.2
17.3 (SPS)	1.42	1.4	0.5	0.15
19.6	1.22	1.4	0.5	0.15
27	1.0	1.2	0.5	0.12
39	0.9	1.0	0.7	0.08
62.4	0.7	1.0	0.7	0.08
200	0.4	1.0	1.0	0.08

Model tuned by matching with existing experimental data from SPS and BES-I RHIC

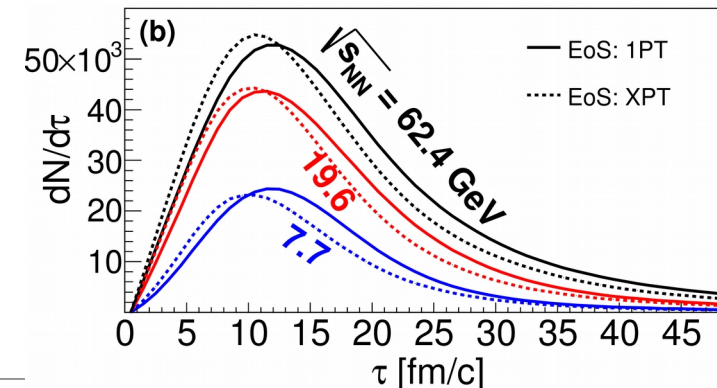
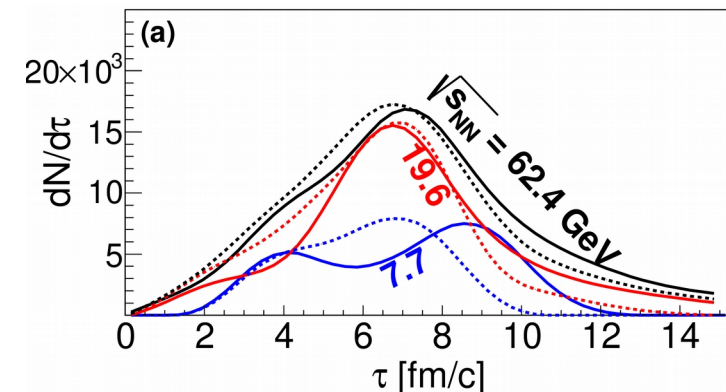
EoS to be used in the model

- Chiral EoS - crossover transition
J. Steinheimer et al., J. Phys. G 38, 035001 (2011)
- Hadron Gas + Bag Model 1st-order phase transition
P. F. Kolb et al., Phys.Rev. C 62, 054909 (2000)

Hydrodynamic phase lasts longer with 1PT, especially at lower energies but cascade smears this difference.

Pion emission time

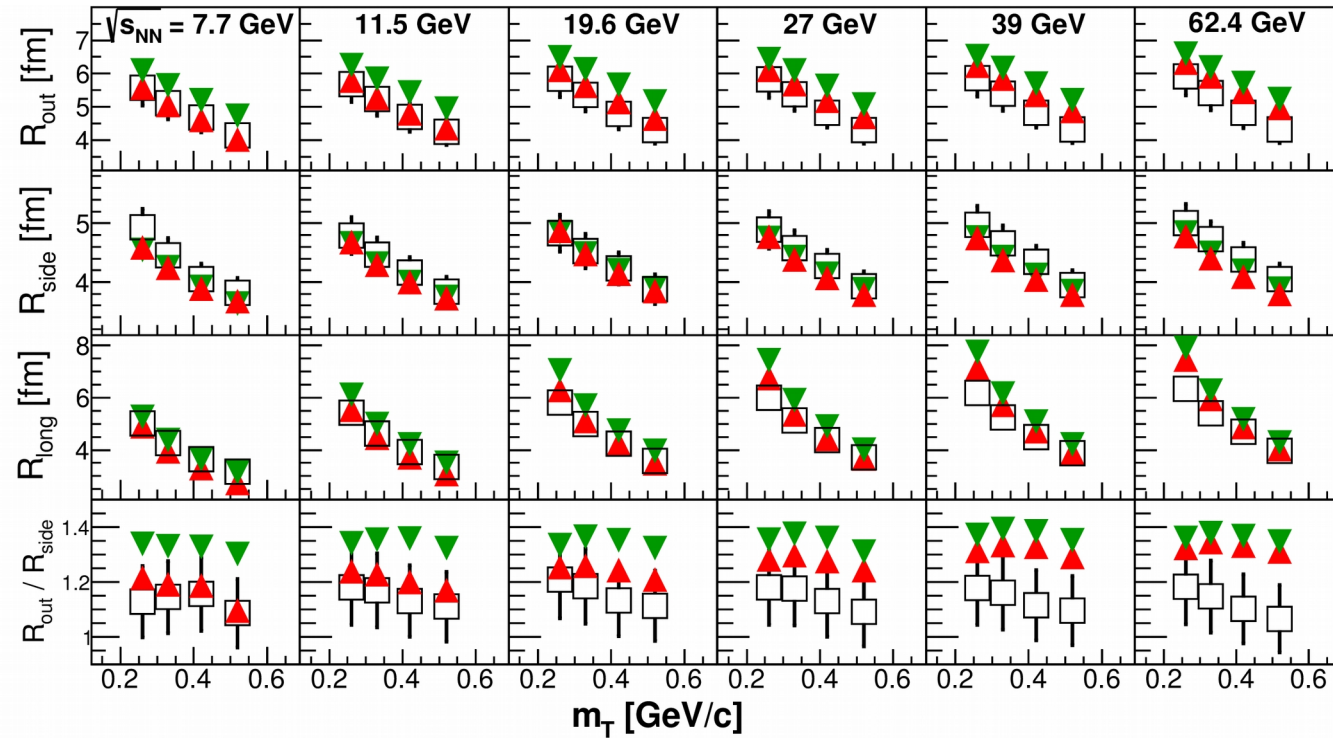
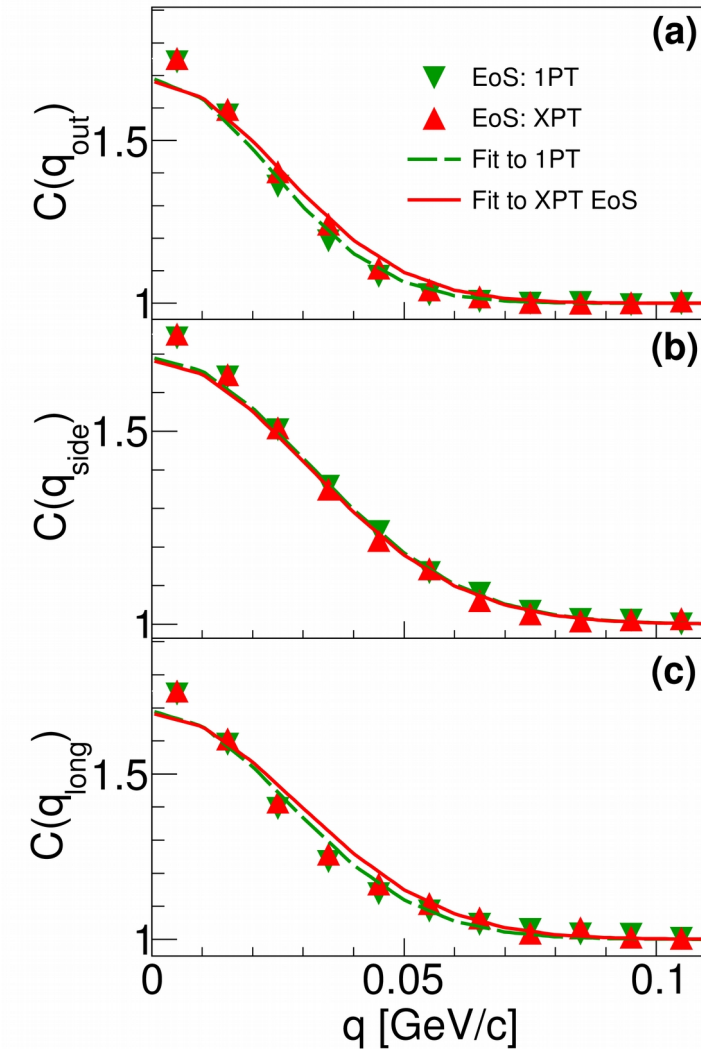
- (a) - after hydrodynamic phase
- (b) - after cascade



3D Pion radii versus m_T with vHLLE+UrQMD

Comparison of extracted radii with the STAR data [PRC 96, 024911(2017)]

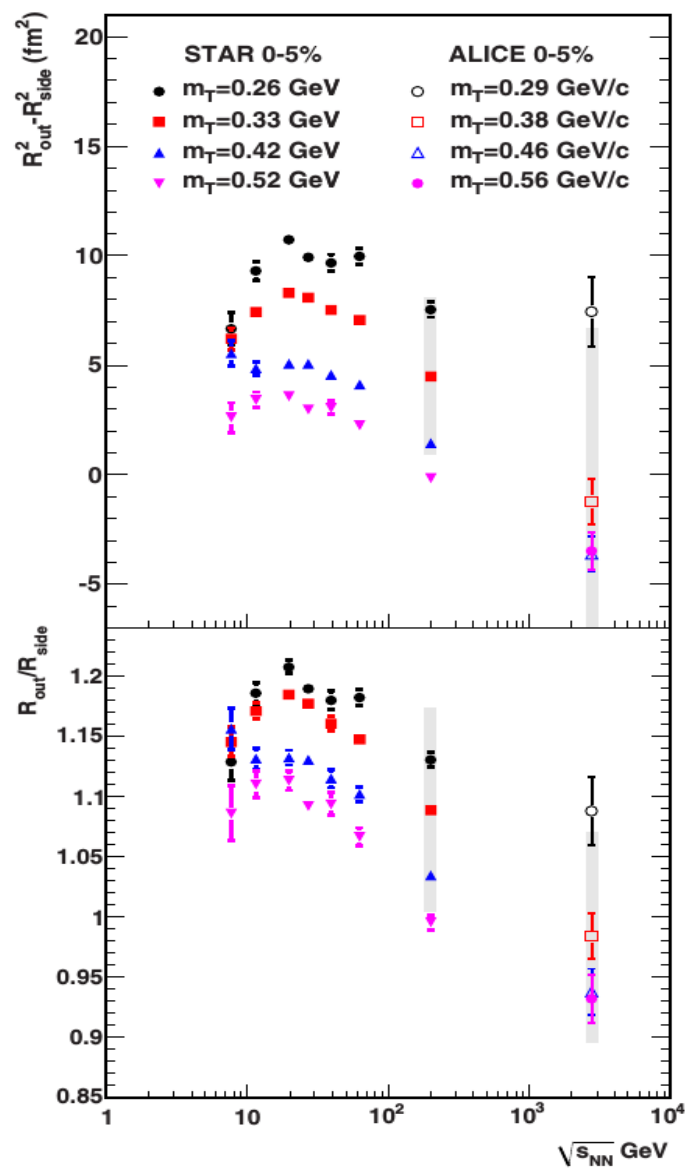
Model CF



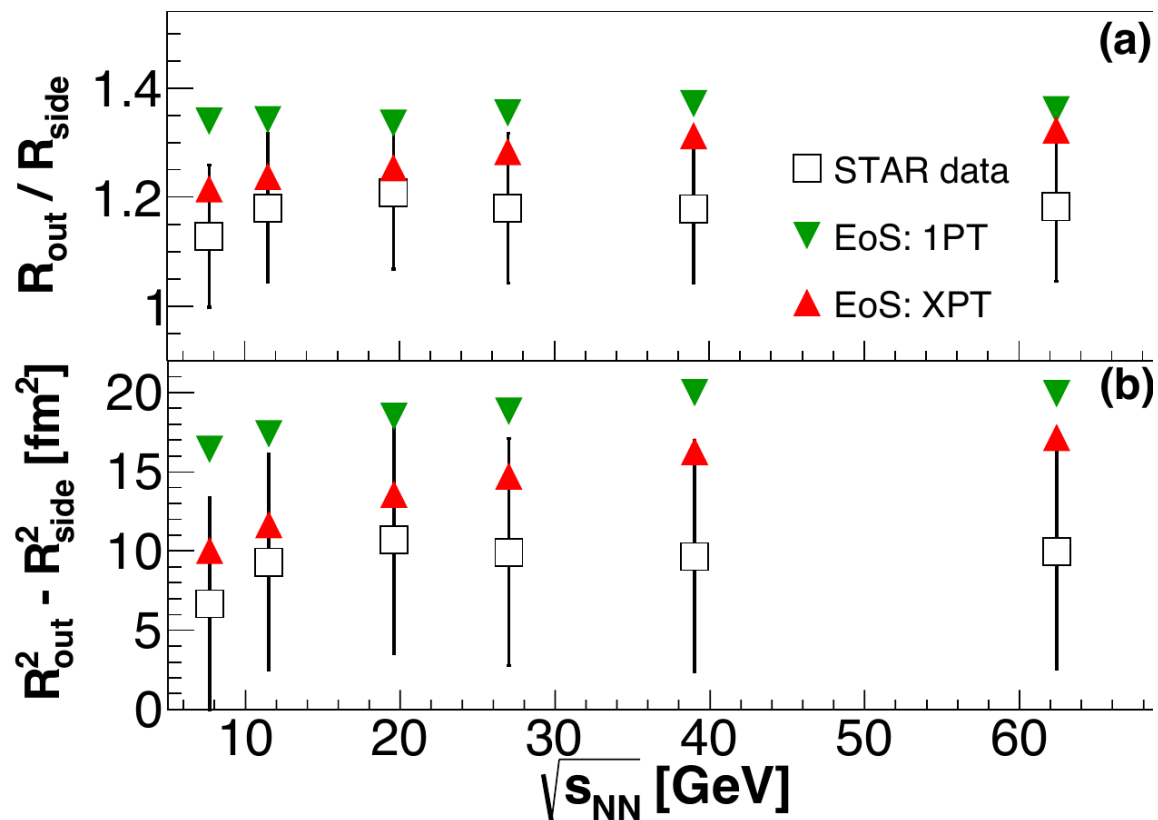
- Femtoscopy radii are sensitive to the type of the phase transition
- **Crossover EoS** does better job at lowest collision energies.
- R_{out} (XPT) at high energies and R_{out} (1PT) at all energies are slightly overestimated
- $R_{\text{out, long}}$ (1PT) $>$ $R_{\text{out, long}}$ (XPT) by value of $\sim 1-2$ fm.

$R_{\text{out}}/R_{\text{side}}$ with vHLLE + UrQMD model

Exp. data: $R_{\text{out}}/R_{\text{side}}$ and $R_{\text{out}}^2 - R_{\text{side}}^2$ as a function of $\sqrt{s_{\text{NN}}}$ at a fixed m_{T} demonstrate a wide maximum near $\sqrt{s_{\text{NN}}} \approx 20$ GeV

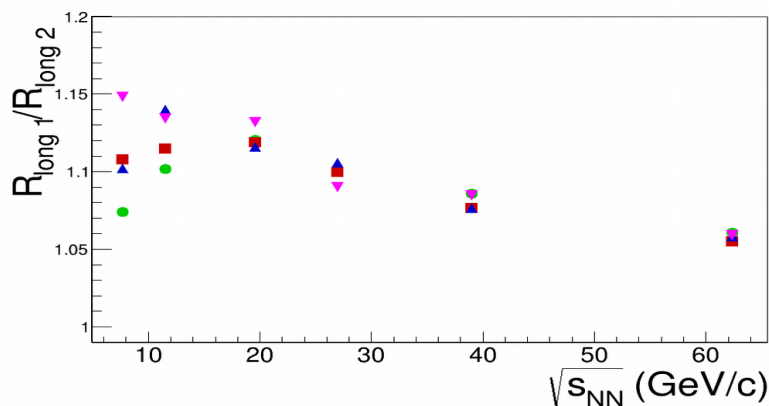
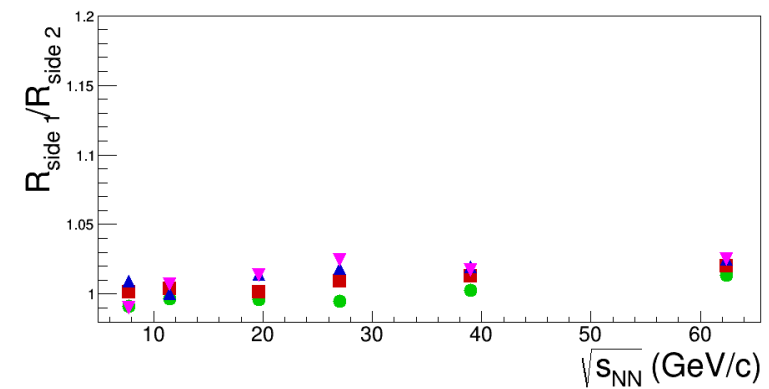
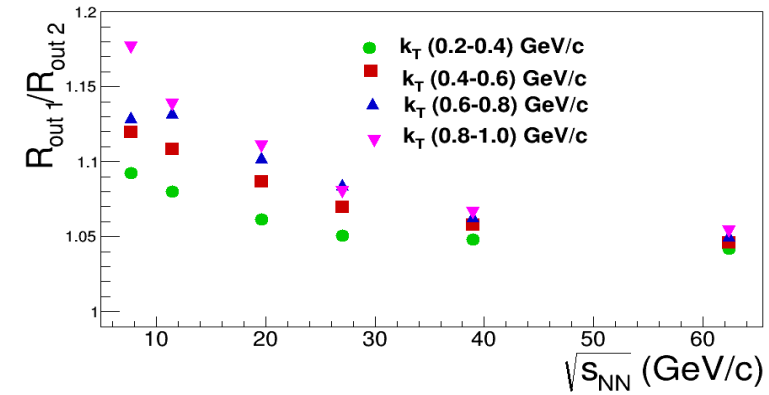


Present vHLLE+UrQMD calculations:



- $R_{\text{out}}/R_{\text{side}}$ (XPT) agrees with almost all STAR data points within rather large systematic errors, while $R_{\text{out}}/R_{\text{side}}$ (1PT) overestimates the data.
- XPT – a monotonic increase in both quantities

Ratio of $R_{\text{out,side,long}}(1\text{PT})/R_{\text{out,side,long}}(\text{XPT})$ vs. $\sqrt{s_{\text{NN}}}$



- Pion k_T divided into 4 bins
- R_{side} ratio practically coincide for both scenarios
- R_{out} and R_{long} ratios for 1PT EoS are greater than for XPT EoS and demonstrating a strong k_T -dependence at low energy
- The difference comes from a **weaker transverse flow** developed in the fluid phase with 1PT EoS as compared to XPT EoS and its longer lifetime in 1PT EoS

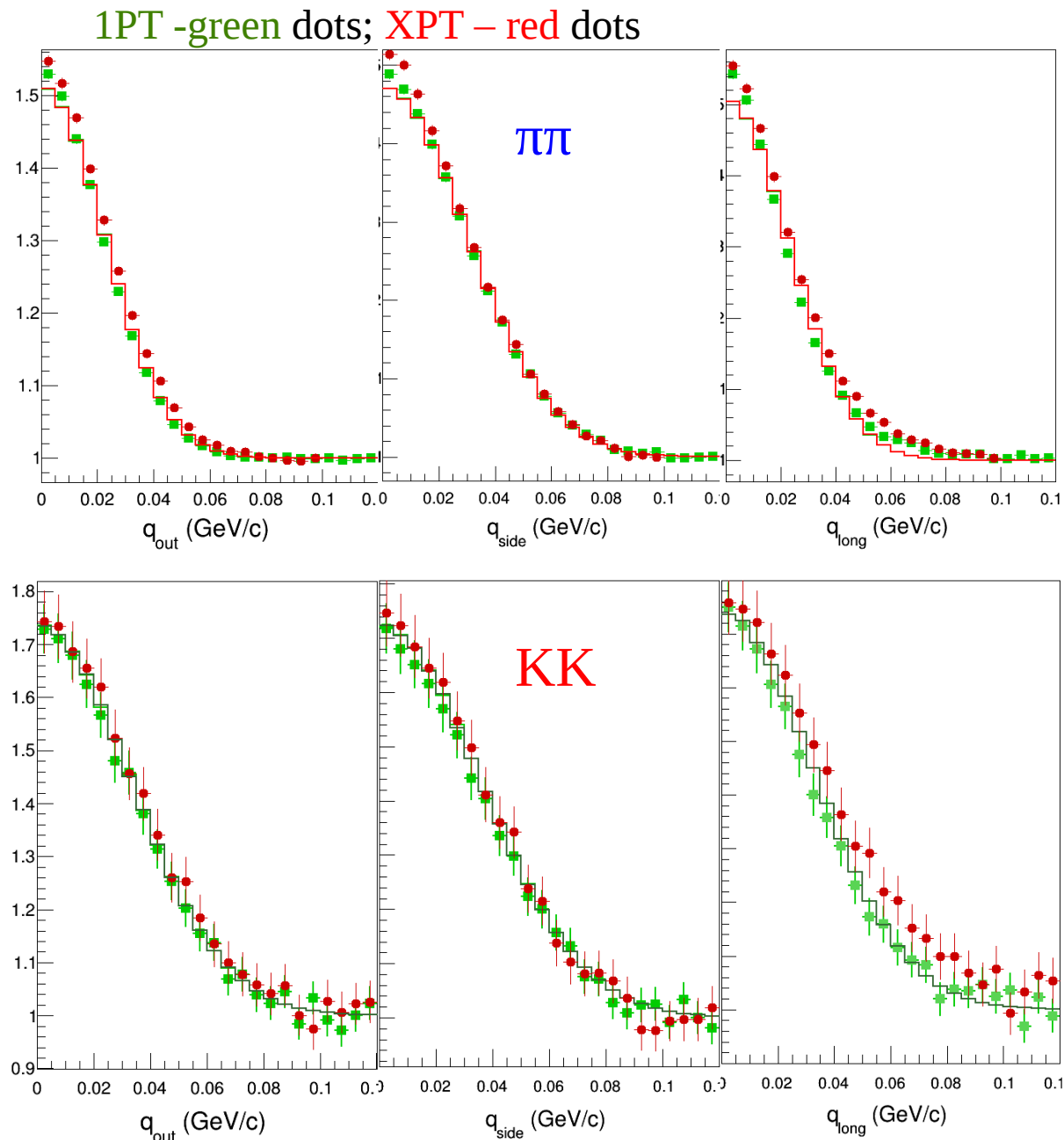
Kaon correlation functions with vHLE+UrQMD (NEW!)

Analysis:

- Au+Au, $\sqrt{s_{NN}} = 11.5$ GeV
- $N_{\text{events}} \approx 4 \cdot 10^5$
- Standard 3D Gaussian fit used
- Our, side, long projections

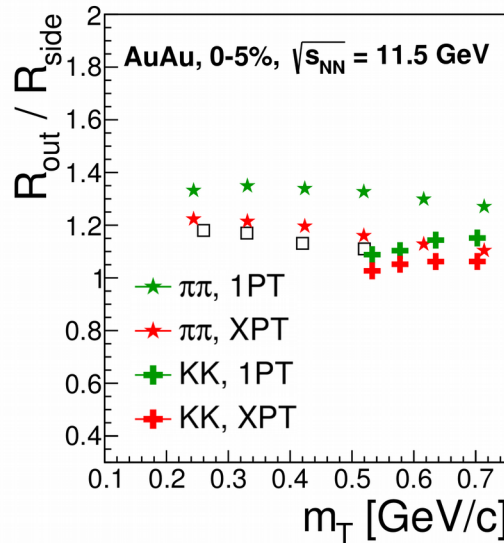
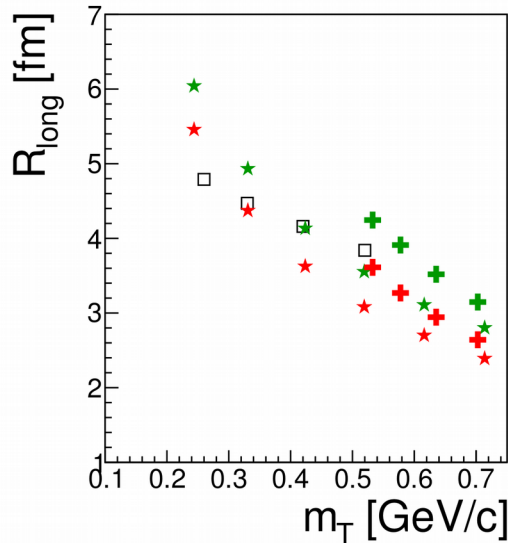
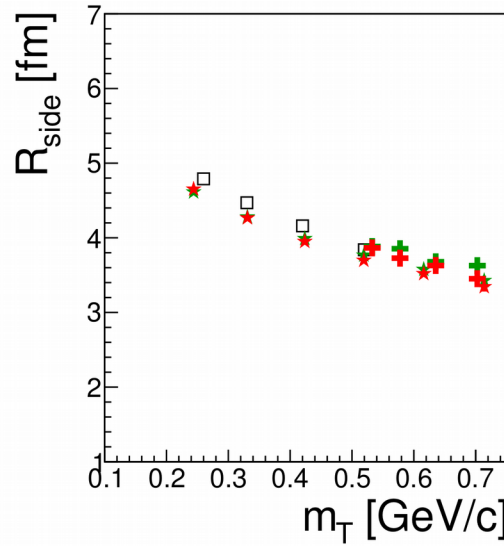
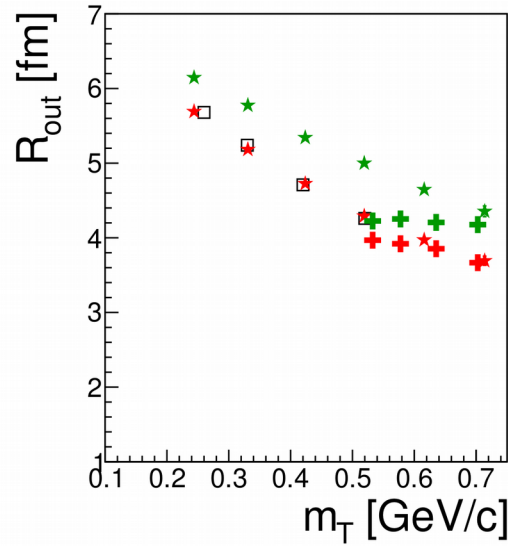
- Projections of 3D kaon correlation functions on out-side-long directions are more Gaussian

- XPT CF projections on long direction are visibly wider than 1PT especially for kaons



Radii π and K vs. m_T with vHLE+UrQMD

1PT -green dots; XPT - red dots



- Au+Au, $\sqrt{s_{NN}} = 11.5$ GeV
- As well as for π , kaon out and long radii greater for 1PT than for XPT
- Approximate m_T -scaling for pions and kaons observed only for “side” radii
- R_{out} almost flat for 1PT
- $R_{long}(KK)$ is greater than $R_{long}(\pi\pi)$ kaons on average emitted later than pions
- $R_{out}/R_{side}(KK)$ for kaons is less than for pions
- Approximately the same result is for Au+Au $\sqrt{s_{NN}} = 7.7$ GeV
- It is important to measure both kaons and pions

Conclusions

- Hydro phase lasts longer with 1PT.
- vHLLE+UrQMD with XPT-scenario describes BES-I STAR femtoscopy radii at $\sqrt{s_{NN}} = 7.7, 11.5$ GeV better than the 1PT-scenario.
- R_{long} for 1PT is greater than for XPT.
- $R_{\text{out}}/R_{\text{side}}$ for 1PT also is greater than for XPT.
- First results with kaon femtoscopy look promising and this study is planned to be continued.

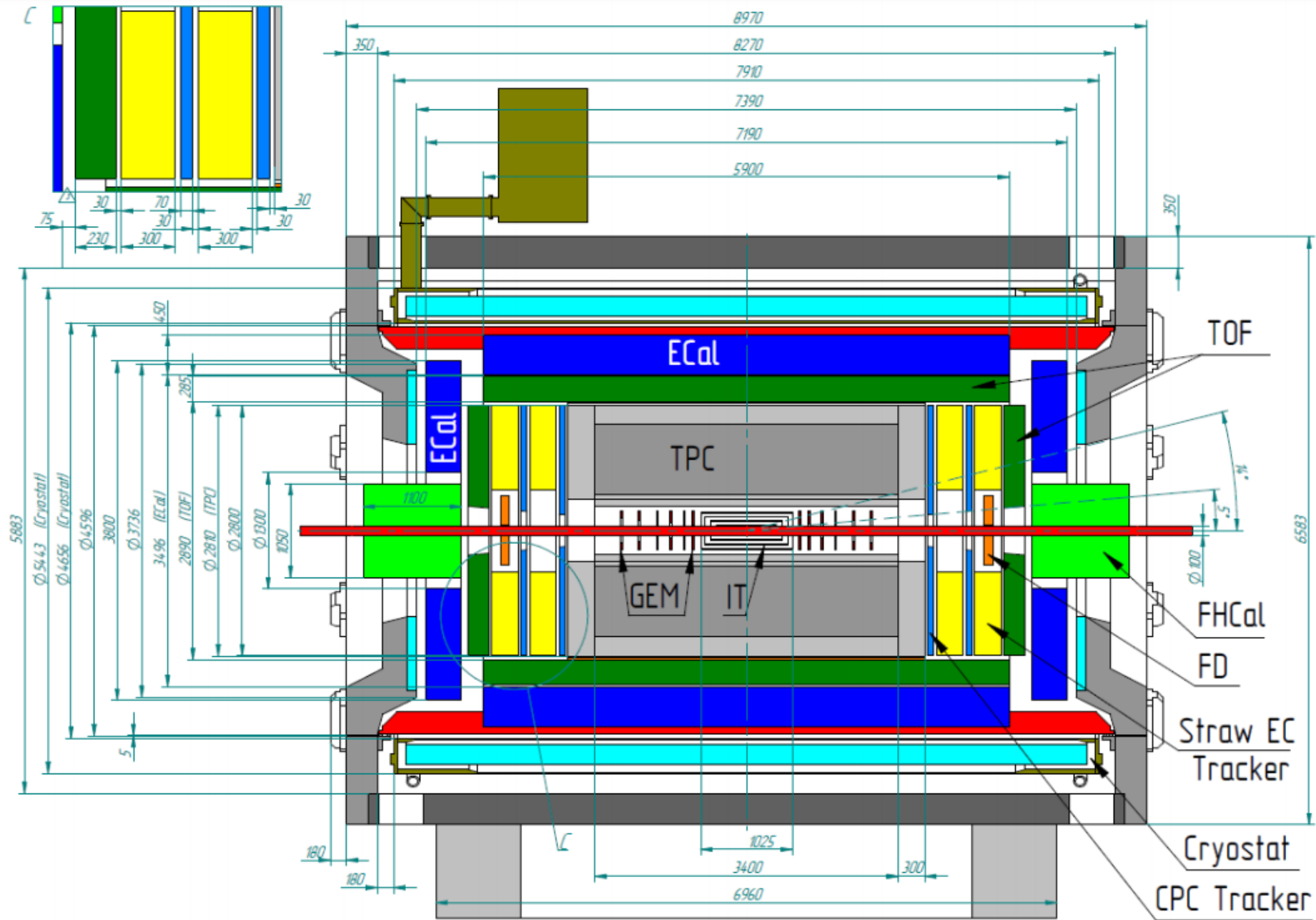
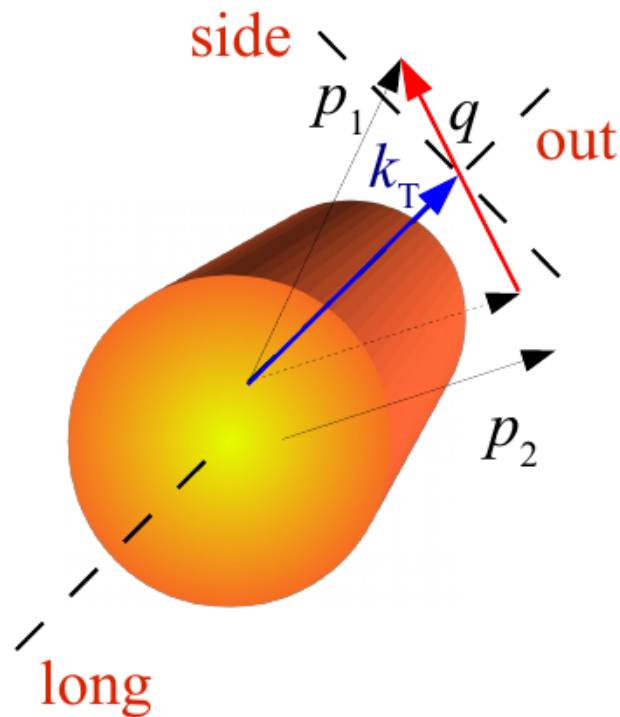


Fig. 2: Side view of the MPD experiment with indicated subsystem dimensions.

LCMS reference frame



$$m_T = \sqrt{k_T^2 + m_\pi^2}$$

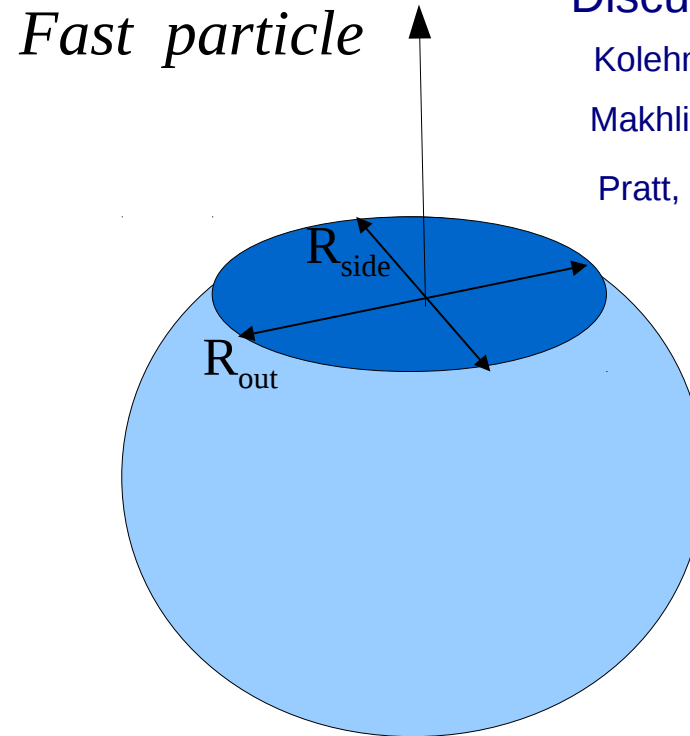
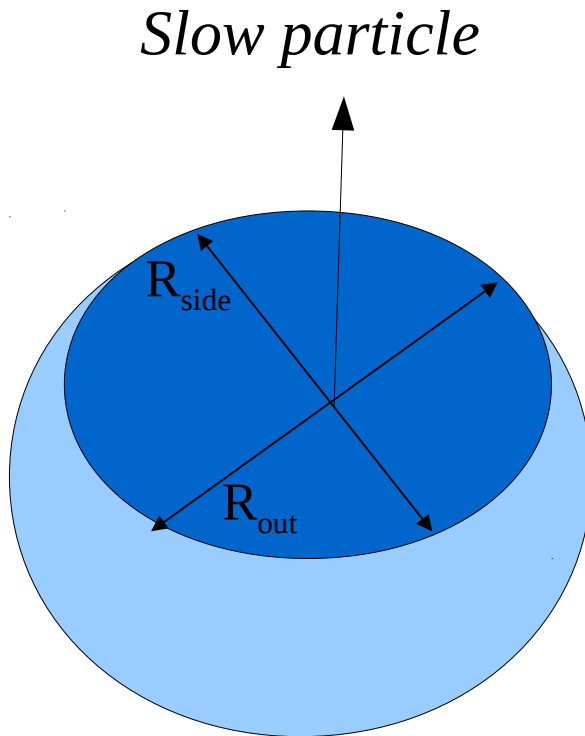
Longitudinally Co-Moving System (LCMS):

$$p_{1,long} = -p_{2,long}$$

- For charged pions measurement in 3 dimensions, giving 3 independent sizes in Longitudinally Co-Moving System
- The Bertsch-Pratt decomposition of q :
 - Long along the beam: sensitive to longitudinal dynamics and evolution time
 - Out along k_T : sensitive to geometrical size, emission time and space-time correlation
 - Side perpendicular to Long and Out: sensitive to geometrical size
- For statistically challenged analyses, measurement in one dimension (giving only one size) in Pair Rest Frame

Femtoscscopy with expanding source $\rightarrow m_T$ -dependence

- $\mathbf{x-p}$ correlations \rightarrow interference dominated by particles from nearby emitters.
- Interference probes only parts of the source at close momenta – **homogeneity regions**.
- Longitudinal and transverse expansion of the source \rightarrow significant reduction of the radii with increasing pair velocity, consequently with k_T (or $m_T = (m^2 + k_T^2)^{1/2}$)



Discussed in e.g.:
 Kolehmainen, Gyulassy'86
 Makhlin-Sinyukov'87
 Pratt, Csörgö, Zimanyi'90

$$R_{\text{side}} \sim R / (1 + m_T \beta_T^2 / T)^{1/2}$$

$$R_{\text{long}} = \tau (T / m_T)^{1/2}$$

$$R_{\text{out}}^2 \sim R_{\text{side}}^2 + 1/2 (T / m_T)^2 \beta_T^2 \tau^2$$

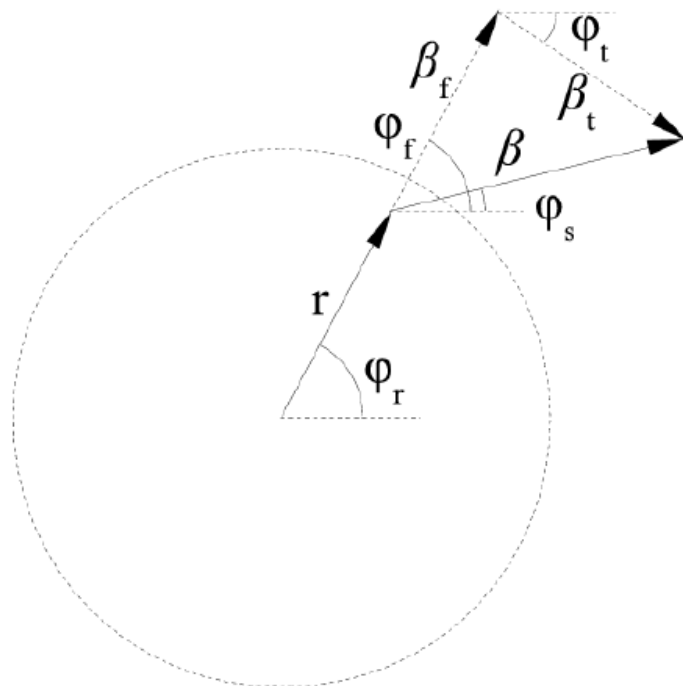
β_T collective transverse flow

assuming a longitudinal boost invariant expansion

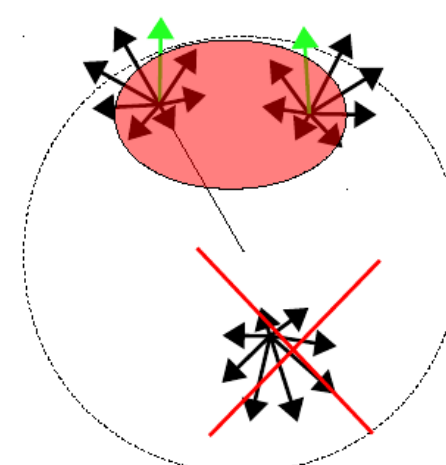
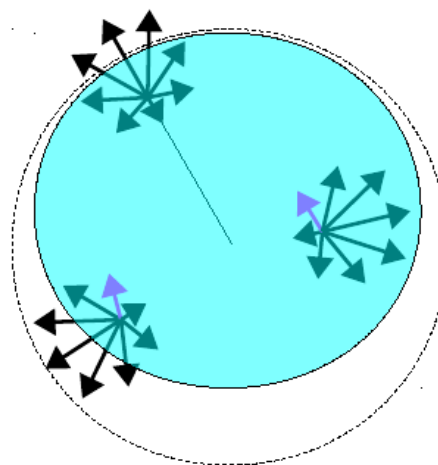
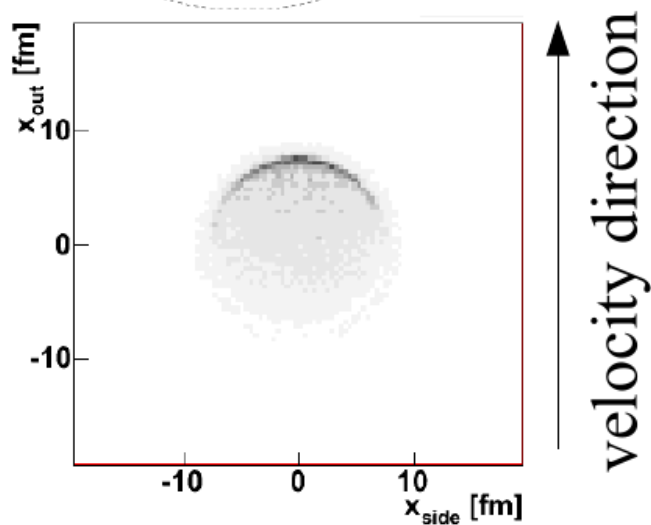
Expanding source

Interference probes only parts of the source at close momenta – **homogeneity regions**.

[Yu.M. Sinyukov, Nucl. Phys. A 566, 589 (1994);]



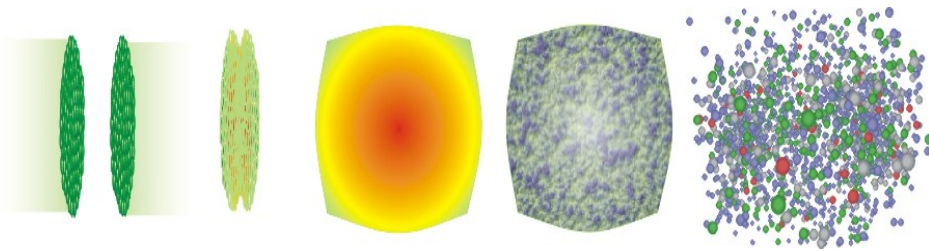
- A particle emitted from a medium will have a collective velocity β_f and a thermal (random) one β_t
- As observed p_T grows, the region from where pairs with small relative momentum can be emitted gets smaller and shifted to the outside of the source



Femtoscscopy: physics motivation

HI collisions

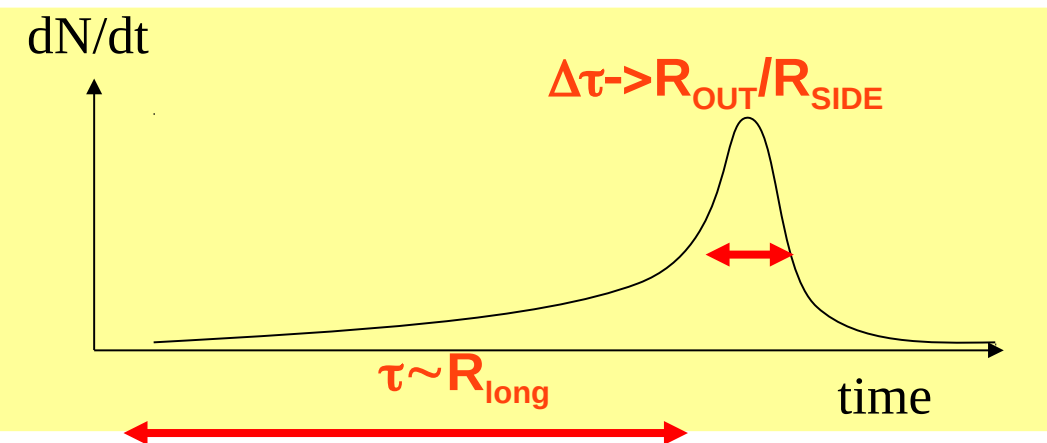
- Measure the size of the homogeneity region from which the volume of the QGP can be inferred
- Study of radii dependence on transverse momentum \rightarrow manifestation of collective motion of matter
- Study of transverse mass dependence for different particle types (π , K, p , ...) - additional confirmation of the hydrodynamic type of expansion: m_T scaling & asymmetries
- Study of source shape at freeze-out: az-femtoscscopy



pp collisions

- Study space-time characteristics of particle production in “elementary process”
- Multiplicities, comparable to peripheral AA collisions: collectivity in pp as in AA ?

Constraints on model parameters.



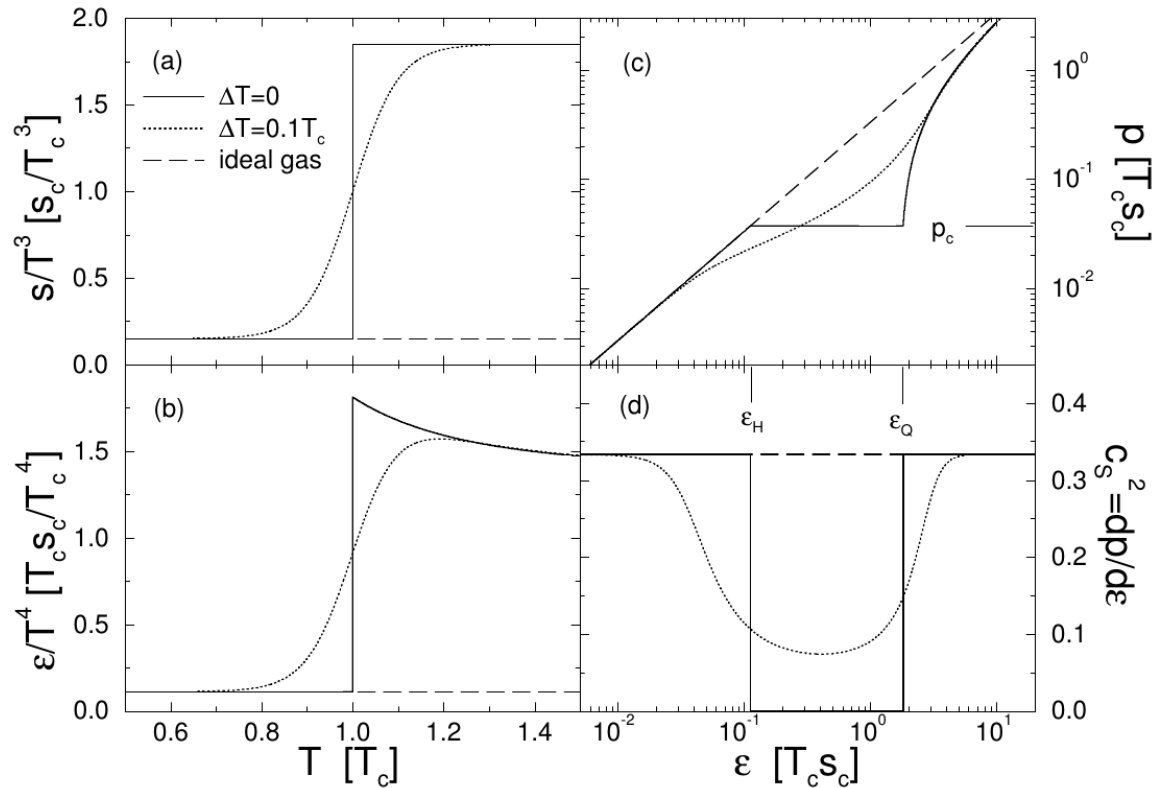


Fig. 1: (a) the entropy density divided by T^3 (in units of s_c/T_c^3), (b) the energy density divided by T^4 (in units of $T_c s_c/T_c^4$) as functions of temperature (in units of T_c), (c) the pressure (in units of $T_c s_c$), (d) the square of the velocity of sound as functions of energy density (in units of $T_c s_c$). The solid lines correspond to $\Delta T = 0$, the dotted curves $\Delta T = 0.1 T_c$. Quantities for the ideal gas equation of state (with d_H degrees of freedom) are represented by dashed lines. The ratio of degrees of freedom in the QGP to those in the hadronic phase is $d_Q/d_H = 37/3$. The critical enthalpy density is $T_c s_c \simeq 0.75 \text{ GeV fm}^{-3}$ for \simeq the case $d_Q = 37, d_H = 3$.

$$\tau_0 = 2R / \sqrt{(\sqrt{s_{\text{NN}}}/2m_N)^2 - 1},$$

Minimal time of starting hydrodynamic evolution:
average time for the two colliding nuclei to completely
pass through each other.

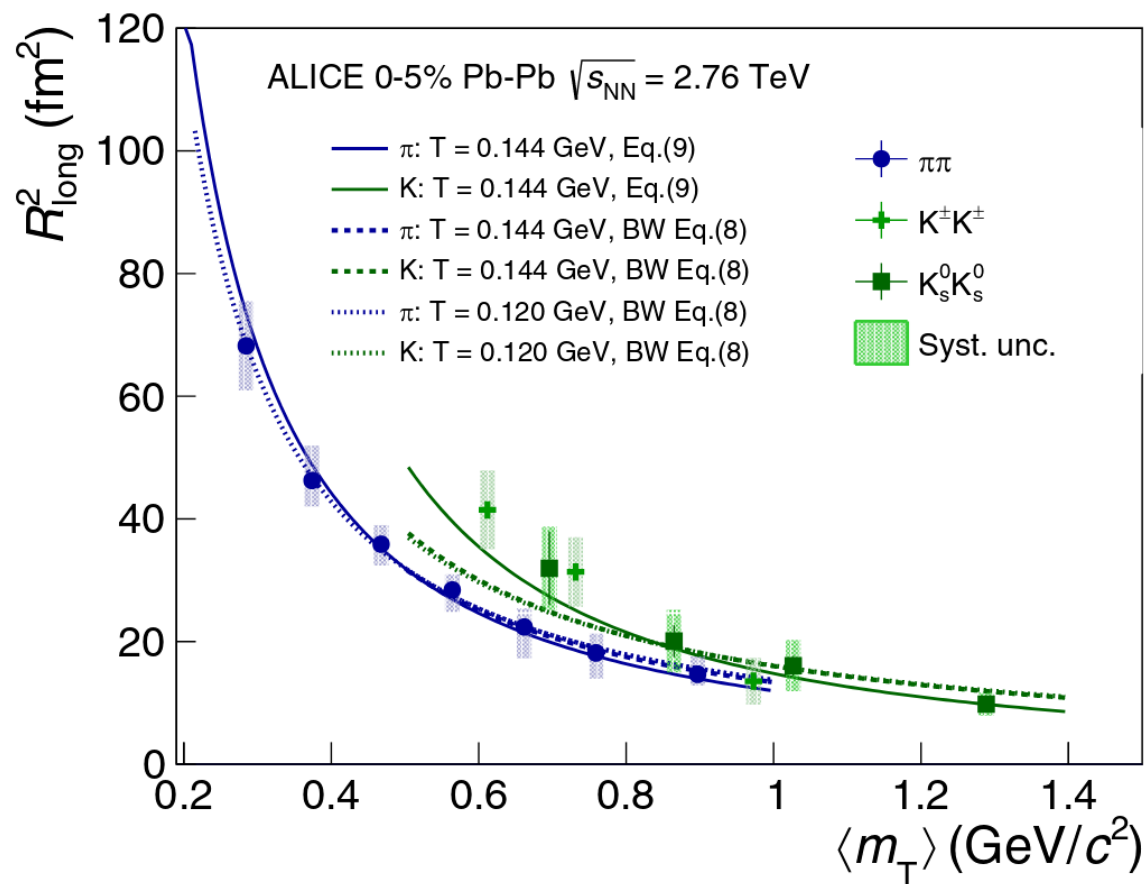
At $\tau = \tau_0$ energy, momentum and baryon/electric charges of hadrons are distributed to fluid cells ijk around each hadron's position according to Gaussian profiles:

$$\begin{aligned} \Delta P_{ijk}^\alpha &= P^\alpha \cdot C \cdot \exp\left(-\frac{\Delta x_i^2 + \Delta y_j^2}{R_\perp^2} - \frac{\Delta \eta_k^2}{R_\eta^2} \gamma_\eta^2 \tau_0^2\right) \quad (2) \\ \Delta N_{ijk}^0 &= N^0 \cdot C \cdot \exp\left(-\frac{\Delta x_i^2 + \Delta y_j^2}{R_\perp^2} - \frac{\Delta \eta_k^2}{R_\eta^2} \gamma_\eta^2 \tau_0^2\right), \quad (3) \end{aligned}$$

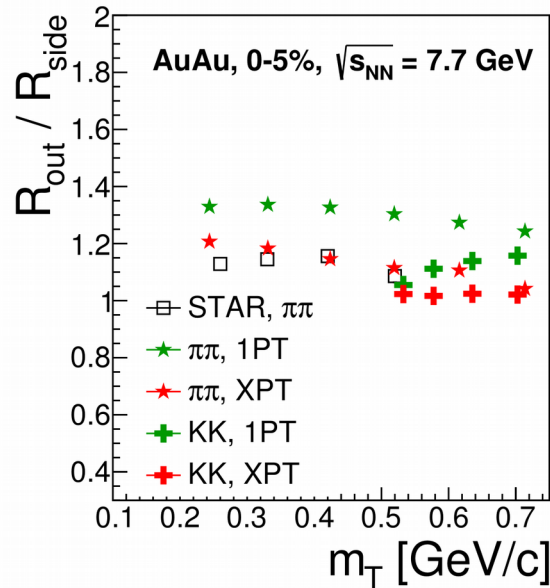
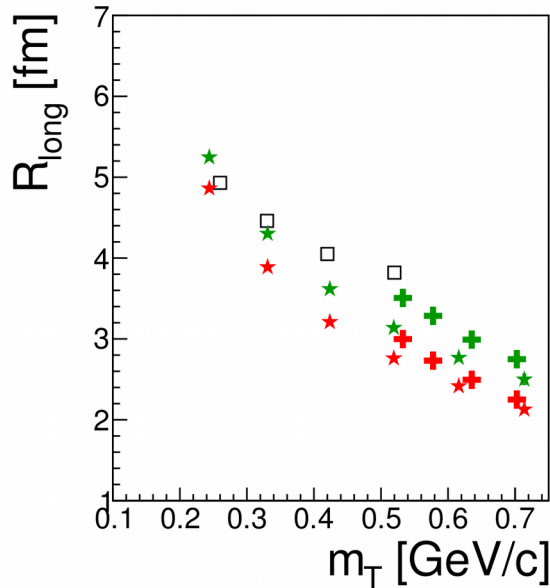
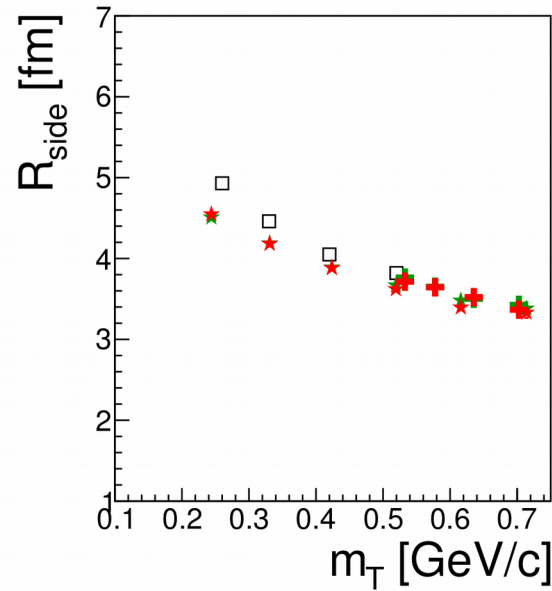
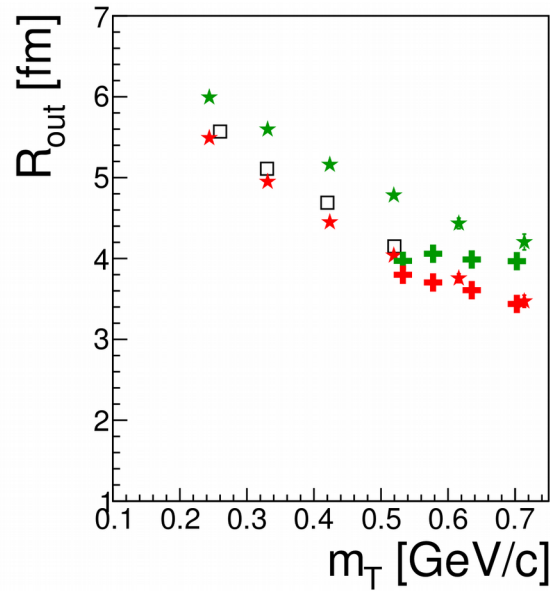
where P^α and N^0 are 4-momentum and charge of a hadron, $\{\Delta x_i, \Delta y_j, \Delta \eta_k\}$ are the distances between hadron's position and center of a hydro cell ijk in each direction, $\gamma_\eta = \cosh(y_p - \eta)$ is the longitudinal Lorentz factor of the hadron as seen in a frame moving with the rapidity η , and C is a normalization constant. The normalization constant C is calculated so that the discrete sum of energy depositions to the hydrodynamic cells equals to the energy of the hadron. The width parameters R_\perp and R_η control granularity of the produced initial state.

Emission delay in ALICE data

- ALICE kaon data in hydro-based parameterization: kaons emitted on average later than pions.
- It comes from rescattering via K^* resonance
- $R_{\text{long}}^2 \sim \tau / \sqrt{m_T}$
- Measured values: $\tau_{\pi} = 9.5 \pm 0.2 \text{ fm}/c$
 $\tau_K = 11.6 \pm 0.1 \text{ fm}/c$



Radii π and K vs. m_T with vHLLE+UrQMD (7.7GeV)



- AuAu, $\sqrt{s_{\text{NN}}} = 7.7$ GeV
- As well as for π kaon out and long radii greater for 1PT than for XPT
- Approximate m_T scaling for pions and kaons observed only for “side” radii